European Journal of Nuclear Medicine and Molecular Imaging (2018) 45:1108–1118
https://doi.org/10.1007/s00259-018-3963-x

ORIGINAL ARTICLE

Cardiac denervation evidenced by MIBG occurs earlier than amyloid deposits detection by diphosphonate scintigraphy in TTR mutation carriers

Eve Piekarski[1] · Renata Chequer[1] · Vincent Algalarrondo[2,3] · Ludivine Eliahou[2,3] · Besma Mahida[1] · Jonathan Vigne[1] · David Adams[3,4] · Michel S. Slama[2,3] · Dominique Le Guludec[1] · Francois Rouzet[1]

Received: 28 September 2017 / Accepted: 24 January 2018 / Published online: 6 March 2018

Abstract

Purpose Cardiac involvement in familial transthyretin (TTR) amyloidosis is of major prognostic value, and the development of early-diagnostic tools that could trigger the use of new disease-modifying treatments is crucial. The aim of our study was to compare the respective contributions of ^{99m}Tc-diphosphonate scintigraphy (DPD, detecting amyloid deposits) and ^{123}I-MIBG (MIBG, assessing cardiac sympathetic denervation) in patients with genetically proven TTR mutation referred for the assessment of cardiac involvement.

Methods We prospectively studied 75 consecutive patients (classified as symptomatic or asymptomatic carriers), using clinical evaluation, biomarkers (troponin and BNP), echocardiography, and nuclear imaging. Patients were classified as having normal heart-to-mediastinum (HMR) MIBG uptake ratio 4 h after injection (defined by HM4 ≥ 1.85) or abnormal HM4 < 1.85, and positive DPD uptake (grade ≥ 1 of Perugini classification) or negative DPD uptake.

Results Among 75 patients, 49 (65%) presented with scintigraphic sympathetic cardiac denervation and 29 (39%) with myocardial diphosphonate uptake. When MIBG was normal, DPD was negative except for two patients. Age was an independent predictor of abnormal scintigraphic result of both MIBG and DPD (HR 1.08 and 1.15 respectively), whereas echocardiographic-derived indicators of increased left ventricular filling pressure (E/e' ratio) was an independent predictor of abnormal MIBG (HR 1.33) and global longitudinal strain of positive DPD (HR 1.45). In asymptomatic patients ($n = 31$), MIBG was abnormal in 48% ($n = 15$) among whom 50% had a normal DPD; all those with a normal MIBG ($n = 16$) had a normal DPD.

Conclusions In TTR mutation carriers, cardiac sympathetic denervation evidenced by decreased MIBG uptake is detected earlier than amyloid burden evidenced by DPD. These results raise the possibility of a diagnostic role for MIBG scintigraphy at an early stage of cardiac involvement in TTR-mutated carriers, in addition to its well-established prognostic value.

Keywords Amyloidosis · Transthyretin · Cardiac amyloidosis · MIBG scintigraphy · Diphosphonate scintigraphy

Eve Piekarski and Renata Chequer contributed equally to this work.

Electronic supplementary material The online version of this article (https://doi.org/10.1007/s00259-018-3963-x) contains supplementary material, which is available to authorized users.

✉ Francois Rouzet
francois.rouzet@aphp.fr

[1] Nuclear Medicine Department, Bichat Claude Bernard Hospital, Assistance Publique Hôpitaux de Paris (AP-HP), DHU FIRE, Inserm UMR-S 1148, Paris Diderot University, Paris, France

[2] Cardiology Department, Antoine Béclère Hospital, AP-HP, Paris-Sud University, Clamart, France

[3] French Referent Center for Rare Diseases for FAP (Familial Amyloid Polyneuropathy) (CRMR-NNERF), Bicêtre Hospital, Le Kremlin-Bicêtre, France

[4] Neurology Department, AP-HP, Paris-Sud University, Le Kremlin-Bicêtre, France

Introduction

Hereditary transthyretin (TTR) amyloidosis is a systemic disease due to a mutation of the gene responsible for the synthesis of TTR [1]. This results in synthesis of an unstable form of TTR, which unfolds and results in monomer, hexamer, and amyloid fiber accumulation in the peripheral nervous system, the heart, the kidneys, and the eyes, with a preferential organ affinity depending on the mutation. More than 100 mutations have been described. Liver transplantation [2, 3] is the reference treatment for the neuropathy, but new treatments such as TTR stabilizers, antisense oligonucleotides, or small interfering RNA are under development [4–7]. As amyloid deposits result in nearly irreversible end-organ damage, future patient care will require both an efficient treatment and a very early diagnosis of organ involvement, before severe dysfunction. This is particularly true with regard to cardiac involvement [8], combining infiltrative cardiomyopathy (myocardial thickening by amyloid deposits, restrictive heart failure with preserved ejection fraction), conductive abnormalities, and cardiac sympathetic and parasympathetic denervation, which is of major prognostic value [9]. The diagnosis of cardiac amyloidosis (CA) among patients with genetically proven TTR mutation relies either on a positive cardiac biopsy, or on the association of a positive peripheral biopsy and evidence of a cardiac infiltration using multimodality imaging. Therefore, there is a great need to develop and evaluate very sensitive non-invasive techniques for the early diagnosis of cardiac TTR amyloidosis [5, 6, 10]. Both morphological and functional imaging modalities, such as echocardiography with strain imaging and cardiac magnetic resonance imaging, are used, along with scintigraphy, in a multimodality imaging process to achieve an early and accurate diagnosis [11–13]. Most studies have evaluated the role of diphosphonate scintigraphy, considering its high diagnostic performance and its prognostic value [14–18]. MIBG scintigraphy was only recognized as a major prognostic factor [19, 20], while its diagnostic value was not considered.

The aim of our study was to evaluate the respective contribution of ^{123}I-MIBG (MIBG) and ^{99m}Tc-diphosphonates (DPD) scintigraphies in the diagnosis of cardiac TTR amyloidosis in consecutive patients with genetically proven TTR mutation, either spontaneously or after domino liver transplant (with histological and genetic TTR mutation proof in the donor).

Material and methods

Population

We prospectively included 75 consecutive patients undergoing assessment of cardiac involvement of amyloidosis in the French Reference Center for Amyloidosis (CRMR-NNERF) between October 2011 and June 2015, which underwent both scintigraphies in the nuclear medicine department. Inclusion criteria were as follows: documented genetic TTR mutation or previous domino liver transplantation (DLT) [21], clinically symptomatic or asymptomatic carrier with regard to cardiac, neurologic, or ophthalmic involvement. Patients referred for cardiac evaluation of suspected wild-type (senile) or other types of amyloidosis (AL, AA, ApoA1) were not included. All patients underwent clinical evaluation of their neurological and cardiac condition, including ECG, echocardiography [interventricular septum (IVS) thickness, left ventricular ejection fraction (LVEF), left ventricular filling pressure estimated by the E/e' ratio and global longitudinal strain (GLS)], and evaluation of BNP (normal ≤ 80 pg/l) and troponin T (normal ≤ 0.05 μg/l) serum levels. History of disease-modifying therapies such as liver transplantation, transthyretin stabilizers (tafamidis) or inclusion in prospective studies with patisiran or inotersen were collected.

This study was in compliance with the ethical principles formulated in the Declaration of Helsinki, and all patients granted their written, informed consent to participate in the registry (Commission Nationale de l'Informatique et des Libertés n°1,470,960).

Nuclear imaging procedures

MIBG scintigraphy imaging, definition of normal and threshold values

Drugs suspected of interfering with MIBG uptake were withheld for an adequate period of time before imaging. As previously described [20], MIBG scintigraphy consisted of planar chest anterior and posterior view acquisitions (10-min acquisition on a Symbia T2, Siemens, Erlangen Germany; low-energy high-resolution collimators; matrix size 128 × 128; energy window of 20% centred on the 159-keV photopeak of ^{123}I) 20 min and 4 h after intravenous injection of 3 MBq/kg of ^{123}I-MIBG (after thyroid blockade) and tomoscintigraphic acquisition at 4 h on a CZT camera (D-SPECT, Spectrum Dynamics, Palo Alto, CA, USA; 12 min acquisition). The scan was associated with a myocardial perfusion tracer injection (^{201}thallium) at rest with tomoscintigraphic acquisition on a CZT camera to assess innervation/perfusion mismatch.

Regions of interest were manually drawn on the left ventricle and the upper mediastinum areas, and cardiac MIBG uptake was calculated as the heart-to-mediastinum ratio (HMR). The normal HMR threshold assessed on planar images acquired 4 h after injection (referred to as HM4) has been previously determined in a cohort of 49 TTR mutation carriers (age: 45 ± 14 years, 56% females) without cardiac involvement at clinical, biological, and echocardiographic evaluation on initial presentation and during the 2 years following MIBG

scintigraphy. Their mean HM4 was 2.15 ± 0.15, so cardiac denervation was defined by HM4 < 1.85 (e.g., 2.15 minus 2 SD).

We also determined a lower threshold suggestive of increased risk of adverse events. This threshold was set at 1.4 based on consistent results of two studies. In a TTR amyloidosis population in whom Val30Met mutation was the most frequent, Algalarrondo et al. [20] reported an increased death rate after transplantation in cases of HM4 < 1.4 (5-year survival rate of 64% if HM4 < 1.4 vs 93%, $p < 0.0001$). Similarly, Coutinho et al. [19] reported a dramatic increase of 5-year mortality rate (from < 20% to 50%) when HM4 was < 1.4 in an exclusively Val30Met population. Hence, three subgroups of patients were considered: subgroup A (HM4 ≥ 1.85) with no denervation, subgroup B (1.85 > HM4 ≥ 1.4) with moderate denervation, subgroup C (HM4 < 1.4) with severe denervation. In addition, a segmental analysis of MIBG uptake was performed on SPECT images, in order to determine the location and the extent of sympathetic denervation. As previously described [22], the number of denervated segments was visually graded on a 17-segment model using a 5-level scoring scale (0: normal, 4: no uptake). The total severity score index (SSI) was calculated by summing the scores of individual segments.

Diphosphonate scintigraphy

Diphosphonate scintigraphy consisted of planar thoracic anterior and posterior view acquisition (Symbia T2; Siemens, Erlangen Germany; low-energy high-resolution collimators; matrix size, 256 × 256; energy window of 20% centred on the 140-keV photopeak of ^{99m}Tc) at 3 h after tracer injection (9.5 MBq/kg of ^{99m}Tc-DPD [^{99m}Technetium-3,3,-diphosphono-1,2- propanodicarboxylic acid]), followed by a whole-body planar acquisition and a cardiac tomoscintigraphic acquisition.

Whole-body DPD uptake pattern was graded using the Perugini score [23], with a grading scale ranging from 0 to 3 (0: no cardiac uptake, scintigraphy considered as negative; grade 3: strong cardiac uptake with mild/absent bone uptake) [14]. Since non TTR-related amyloidosis had been ruled out before enrolment, grades 1 to 3 were considered as positive for cardiac amyloidosis deposits. Heart to lung ratio (H/L) was calculated as the ratio between 3D isocount volume of interest generated over the myocardium and a standard volume in right pulmonary base on SPECT images.

Statistical analysis

Continuous variables were expressed by their mean ± standard deviation and compared by use of Student's *t* test or ANOVA followed by the Scheffé's post-hoc test for comparison of more than two groups. Categorical variables were expressed by their percentage and compared by use of Fisher's exact test. Independent predictors of MIBG and DPD cardiac uptake were determined using logistic regression with stepwise selection of variables. In the multivariate model, we did not include the parameter "amyloidosis targeted therapy", since therapy initiation was considered upon a clinical appraisal of the global severity of the disease, dependent on the other patient's characteristics. Linear regression and Pearson correlation coefficients were performed to determine the relation between continuous variables. Statistical analysis was performed using SPSS (IBM) and Medcalc software version 16.4.3 (Ostend, Belgium). A p value < 0.05 was considered as significant.

Results

Study population

A total of 75 consecutive patients were included in the study (Table 1). The most frequent mutation was Val30Met (32 patients, 43%), then Ser77Tyr and Ser77Phe accounted for seven patients each. Ten patients had a history of domino liver transplantation. Most patients were symptomatic (44 patients, 59%), predominantly with neurological symptoms.

Nuclear imaging findings

The delay between MIBG and DPD scans was 6 ± 12 days. In the overall population, MIBG was abnormal in 49 patients (65%), whereas DPD was positive in only 29 (39%) (Table 2). When MIBG was normal, DPD was negative except for two patients (Ala36Pro and Arg34Gly mutations) presenting with grade 3 pattern (other patients' characteristics are detailed in Fig. 1). The relationship between quantitative parameters of MIBG and DPD uptake are presented in Fig. 2.

With regard to rest myocardial perfusion scintigraphy, no patient presenting denervation on MIBG had significant perfusion defect in the corresponding denervated segments, therefore confirming perfusion/innervation mismatch.

We performed a visual regional analysis of MIBG and DPD abnormalities and found different abnormality patterns: whereas MIBG demonstrated preferential abnormalities in the apex and the inferior wall, DPD uptake was most intense in the septum with a relative apical-sparing, as presented in Fig. 3 (and Fig. 1 Supplementary Material) and Table 1 Supplementary material.

Predictors of scintigraphic abnormalities

Table 1 shows that age, amyloidosis targeted therapy, the presence of symptoms, increased BNP level, IVS thickness, altered GLS and E/e' were associated with both MIBG abnormalities and DPD positive uptake, whereas troponin T level

Table 1 Baseline characteristics and results of MIBG and DPD scintigraphy

	Overall population ($n = 75$)	MIBG normal ($n = 26$)	MIBG abnormal ($n = 49$)	*P* value	DPD negative ($n = 46$)	DPD positive ($n = 29$)	*P* value
Age	56 ± 15	46 ± 11	61 ± 14	< 0.0001	50 ± 14	66 ± 10	< 0.0001
Males, *n* (%)	47 (63)	17 (65)	30 (61)	0.6	28 (61)	19 (66)	0.7
Val30Met, *n* (%)	32 (43)	7 (27)	25 (51)	0.05	20 (43)	12 (41)	0.9
DLT, *n* (%)	10 (13)	4 (15)	6 (12)	0.7	8 (17)	2 (7)	0.3
Amyloidosis targeted therapy	30 (40)	5 (20)	25 (51)	0.01	10 (22)	20 (69)	< 0.0001
– Tafamidis / siRNA	19 (25)	2 (8)	17 (35)	0.01	4 (9)	15 (52)	< 0.0001
– Liver transplantation	11 (15)	3 (12)	8 (16)	0.7	6 (13)	5 (17)	0.7
Pacemaker	5 (7)	0	5 (10)	0.2	3 (7)	2 (7)	0.6
Symptoms, *n* (%)	44 (59)	8 (30)	36 (73)	0.006	22 (48)	22 (76)	0.017
– cardiac symptoms only	1	0	1	0.6	0	1	0.3
– cardiac and neurologic symptoms	8	0	8	0.1	4	4	0.9
– neurologic symptoms only	30	8	23	0.3	17	14	0.2
Biology							
– BNP (pg/ml)	108 ± 138	30 ± 43	148 ± 153	< 0.0001	57 ± 82	186 ± 169	0.0003
– Troponin (μg/l)	0.06 ± 0.05	0.04 ± 0.02	0.06 ± 0.06	0.003	0.05 ± 0.05	0.06 ± 0.04	0.2
Echocardiography							
– IVS thickness (mm)	12.6 ± 4.4	9.5 ± 2.5	14.1 ± 4.3	< 0.0001	10.6 ± 3.3	15.6 ± 4	< 0.0001
– LVEF (%)	63 ± 9	64 ± 7	62 ± 10	0.5	65 ± 8	60 ± 9	0.03
– GLS (%)	−16.0 ± 4.8	−18.5 ± 2.0	−14.4 ± 5.3	0.001	−18.3 ± 3.0	−13.2 ± 5.0	< 0.0001
– E/e'	10.8 ± 6.3	7.2 ± 4.2	12.6 ± 6.4	0.0004	8.3 ± 5.0	14.6 ± 6.2	< 0.0001

Values are mean ± SD unless otherwise specified; DLT: domino liver transplant; BNP: brain natriuretic peptide; IVS: interventricular septum; LVEF left ventricular ejection fraction; GLS: global longitudinal strain

was lower in patients with normal MIBG, and LVEF was significantly decreased in patients with positive DPD. Patients with normal MIBG had no or little evidence of cardiac amyloidosis, whereas patients with positive DPD presented markers of biological and functional cardiac dysfunction. On multivariate analysis (Table 3), in addition to patients' age that was a common determinant of abnormal finding both with MIBG and DPD, E/e' was an independent predictor of abnormal MIBG, and altered GLS was an independent predictor of DPD positive uptake.

Semi-quantitative evaluation of MIBG and DPD uptake intensity are provided in Figs. 4 and 5. As shown in Figs. 4 and 5, before the age of 50 only two patients presented DPD uptake, whereas ten had mild cardiac denervation on MIBG and none presented severe denervation.

Subgroup analysis

Asymptomatic patients

In the subgroup of asymptomatic patients ($n = 31$), MIBG was abnormal in 15 (48%). DPD was always negative when MIBG was normal, while DPD was positive in eight out of 15 patients with abnormal MIBG (Table 4). Although asymptomatic patients with abnormal MIBG scintigraphy were older than asymptomatic patients with normal MIBG, patients' age did not make it possible to differentiate those at higher risk of abnormal scan because of an important overlap. The same held true for biological markers and echocardiography findings (Table 4). Regional analysis revealed significant differences of MIBG denervation between asymptomatic and symptomatic

Table 2 Scintigraphic results in the whole population ($n = 75$)

	MIBG normal ($n = 26$)	MIBG abnormal ($n = 49$)
DPD negative ($n = 46$)	24 (32%)	22 (29%)
DPD positive ($n = 29$)	2* (3%)	27 (36%)

*Ala36Pro and Arg34Gly mutations

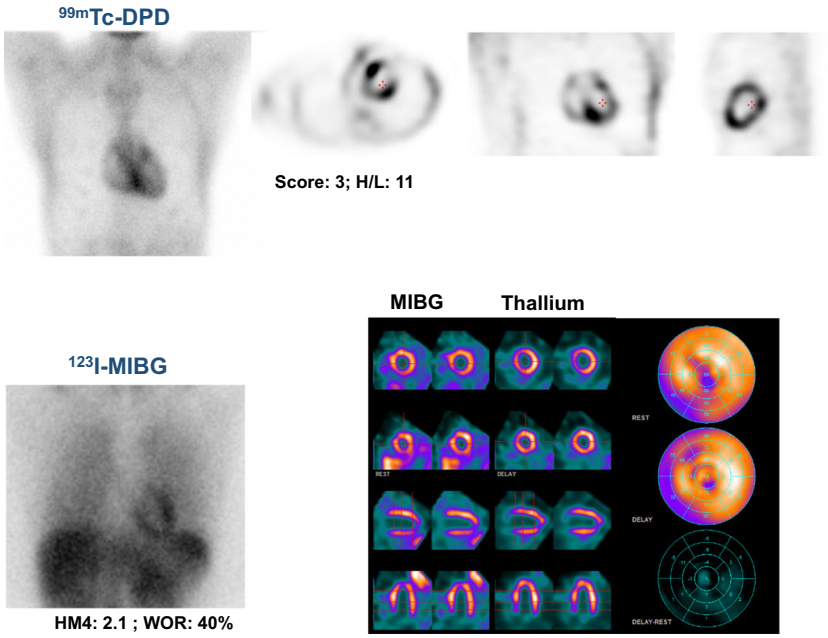

Fig. 1 Example of MIBG and DPD reverse pattern, in a 41-year-old woman with Ala36Pro mutation and ocular involvement. Biological markers were normal (BNP: 9 pg/ml; troponin: 0.04 µg/ml), echocardiography showed interventricular septum thickness of 8 mm, E/e': 5.7, global longitudinal strain: −19, and left ventricular ejection fraction was 59%. MIBG scintigraphy was completely normal with HM4 > 1.85 and the absence of segmental defect, but DPD showed a marked uptake with grade 3. The second patient with a reverse pattern was a 60-year-old man with Arg34Gly mutation, had ocular involvement, left ventricular hypertrophy (interventricular septum thickness: 14 mm) but normal E/e', global longitudinal strain, and left ventricular ejection fraction. Despite normal MIBG scintigraphy (HM4: 1.9, WOR: 34), DPD was grade 3 with H/L: 13.95

patients with more pronounced denervation among symptomatic patients, with a preferential infero-latero-apical denervation pattern in both groups (Table 2 Supplementary Material).

Domino liver transplanted patients

Although domino liver transplanted patients represent a specific subgroup with a shorter exposure time to mutated TTR than carriers of an hereditary mutation, we compared our results in this subgroup and the rest of the population and found no significant differences with regard to scintigraphic results, except for HM20, which was significantly greater in this subgroup (Table 3 Supplementary Material).

MIBG subgroups

The three subgroups defined by the HM4 thresholds presented significant differences with regard to age, symptoms, BNP,

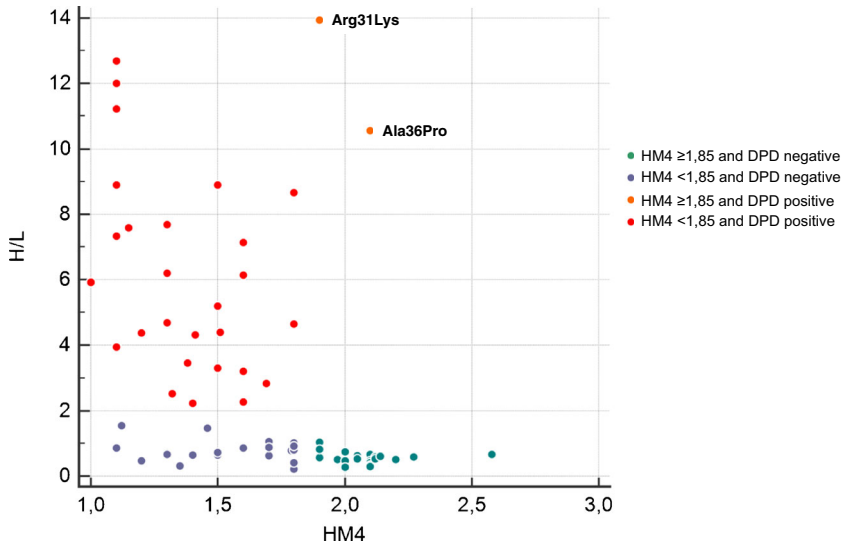

Fig. 2 Relationship between MIBG (HM4) and DPD uptake (H/L ratio) in the study population. There is an inverse relationship between HM4 and H/L (Pearson coefficient $R = -0.41$, $p < 0.001$)

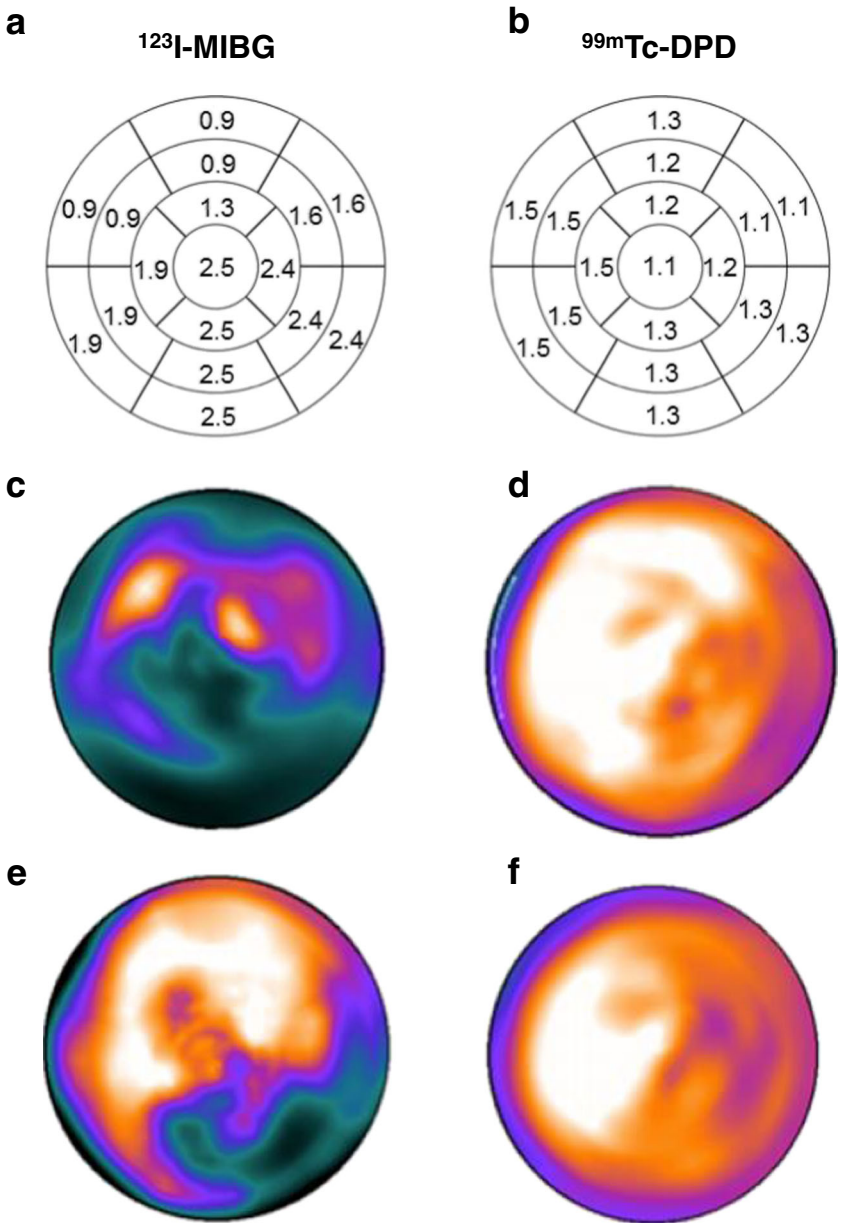

Fig. 3 Results of visual regional analysis of MIBG (**a**) and DPD (**b**) scintigraphic abnormalities using 5-point scales (**a**, for MIBG: 0, normal uptake; 1, mildly reduced uptake; 2, moderately reduced uptake; 3, severely reduced uptake; 4, no uptake; **b**, for DPD: 0, no uptake; 1, low intensity uptake; 2, low to moderately intense uptake; 3, moderate uptake; 4, intense uptake); with examples of diffuse MIBG (**c**) and DPD (**d**) abnormalities in a patient with severe denervation and intensely increased cardiac DPD uptake; and mismatched MIBG (**e**) and DPD (**f**) abnormalities in another patient with moderate denervation and moderate intensity DPD cardiac uptake

echographic findings, positivity of diphosphonates scintigraphy, and H/L: as the HM4 decreased, clinical, biological and echographic parameters were more severely or more frequently impaired (Table 4 Supplementary Material).

Table 3 Independent predictors of abnormal findings on scintigraphy (multivariate analysis)

Predictor	Hazard ratio (95% CI)	*P* value
MIBG abnormal		
– age	1.0803 (1.0072 to 1.1587)	0.03
– E/e'	1.3324 (1.0338 to 1.7173)	0.02
DPD positive		
– age	1.1540 (1.0653 to 1.2500)	0.0004
– GLS	1.4542 (1.1214 to 1.8859)	0.0047

CI: confidence interval. Other abbreviations as in previous tables

Discussion

The present study shows that in TTR mutation carriers, cardiac sympathetic denervation evidenced by decreased MIBG uptake is detected earlier than amyloid burden evidenced by DPD. At the presymptomatic stage, carriers with a normal MIBG scan seem to have a very low likelihood of cardiac involvement, with only a few patients with mild morphological or functional cardiac alterations.

In our study population, a positive DPD uptake was associated with a rather advanced stage of CA. First, age was a

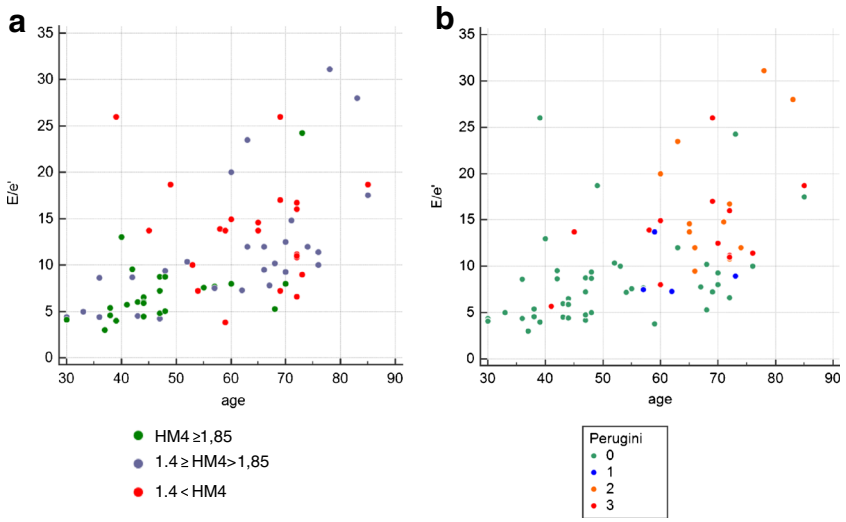

Fig. 4 Combined analysis of the semi-quantitative uptake intensity of MIBG (**a**) and DPD (**b**) according to age and E/e'. Severe denervation is absent in patients < 50 years old and preserved E/e', while mild denervation may be present. There was no significant correlation between either E/e' and HM4 or E/e' and H/L (Pearson coefficient *R* respectively = −0.49 and −0.39, $p < 0.0001$ and = 0.0005)

major determinant of DPD uptake, with only two patients presenting a detectable uptake below 55 years old. Increased LV filling pressure (E/e') was a predictor of abnormal MIBG, while DPD uptake was associated with markers of mild LV systolic dysfunction such as BNP increase, GLS alteration, and LVEF impairment. Diagnostic performances of diphosphonate scintigraphy for TTR amyloidosis have already been demonstrated [14–16], but only a few studies have evaluated its value in asymptomatic patients [18, 24]. Many studies considered a septum thickness ≥ 12 mm as a diagnostic criterion for CA, while this cutoff value does not take into account the existence of a "gray zone". Accordingly, the sensitivity of DPD in cases of cardiac amyloid deposits with septum thickness < 12 mm is not well elucidated. Only rare false-negative diphosphonate exams have been reported, mainly attributed to the type of involved fibrils or to the tracer used [25, 26]. Several scores using semi-quantitative ratios have been described, such as heart/whole body ratio [27–30], heart/skull ratio [27, 31] and two studies ing heart to lung ratios [16, 32], with one [16] finding a correlation between 5-year all-cause mortality rate and heart to lung ratio. The value of a semi-quantitative ratio such as H/L will need to be evaluated in the future.

The prognostic value of MIBG scintigraphy in TTR amyloidosis is well established [19, 20]. However, few studies [19, 33] have evaluated cardiac denervation in asymptomatic carriers or in TTR patients with only echographic abnormalities. In our study population, a mild decrease of MIBG uptake was associated with very early signs of CA, including in the subgroup of asymptomatic carriers. The prognostic significance of a mild decrease of MIBG uptake, without DPD abnormality will need to be assessed in further studies evaluating the occurrence of cardiac events and the potential progression of functional abnormalities. When abnormal, the HM4 decreased with more advanced disease, in keeping with the well-established poor prognosis of patients with severe denervation.

A preliminary study combining MIBG and bone scintigraphy has been performed in 12 patients with symptomatic TTR amyloidosis [34]. Although the MIBG uptake was assessed only qualitatively, the authors reported severe global or segmental denervation in all patients, while bone scintigraphy was positive in only four of them. Interestingly, ten out of 12 patients had had endomyocardial biopsy showing histologic evidence of amyloid deposition, suggesting the lack of sensitivity of bone scintigraphy in this population. Our study confirms the presence of a significant number of patients (nearly one third of the study population) with abnormal MIBG and negative DPD in a greater population sample, and demonstrates that this pattern is even more prominent at the presymptomatic stage, highlighting the potential role of MIBG as an early diagnostic marker of cardiac amyloidosis. In addition, the increase of MIBG uptake associated with regression of autonomic dysfunction after treatment by small interfering RNAs has been reported in a small sample study [35]. Taken together, these results suggest that MIBG could be used in decision-making for early initiation and monitoring of disease-modifying therapies.

Regional analysis of denervation on MIBG and of DPD uptake revealed different patterns, with a predominant denervation of the apex and inferior segments, and a relative apical-sparing pattern on DPD as previously described [36]. Those findings support the hypothesis that two different pathophysiological mechanisms are observed, cardiac denervation with MIBG versus myocardial amyloid deposition, with different locations. The regional DPD uptake is consistent with apical sparing of longitudinal strain observed with echocardiography. The regional MIBG results can be explained on the basis of anatomical and histological studies, demonstrating that sympathetic nerve distribution is heterogeneous among the left ventricular walls, with a preferential distribution among basal segments versus apical segments [37–42]. A study

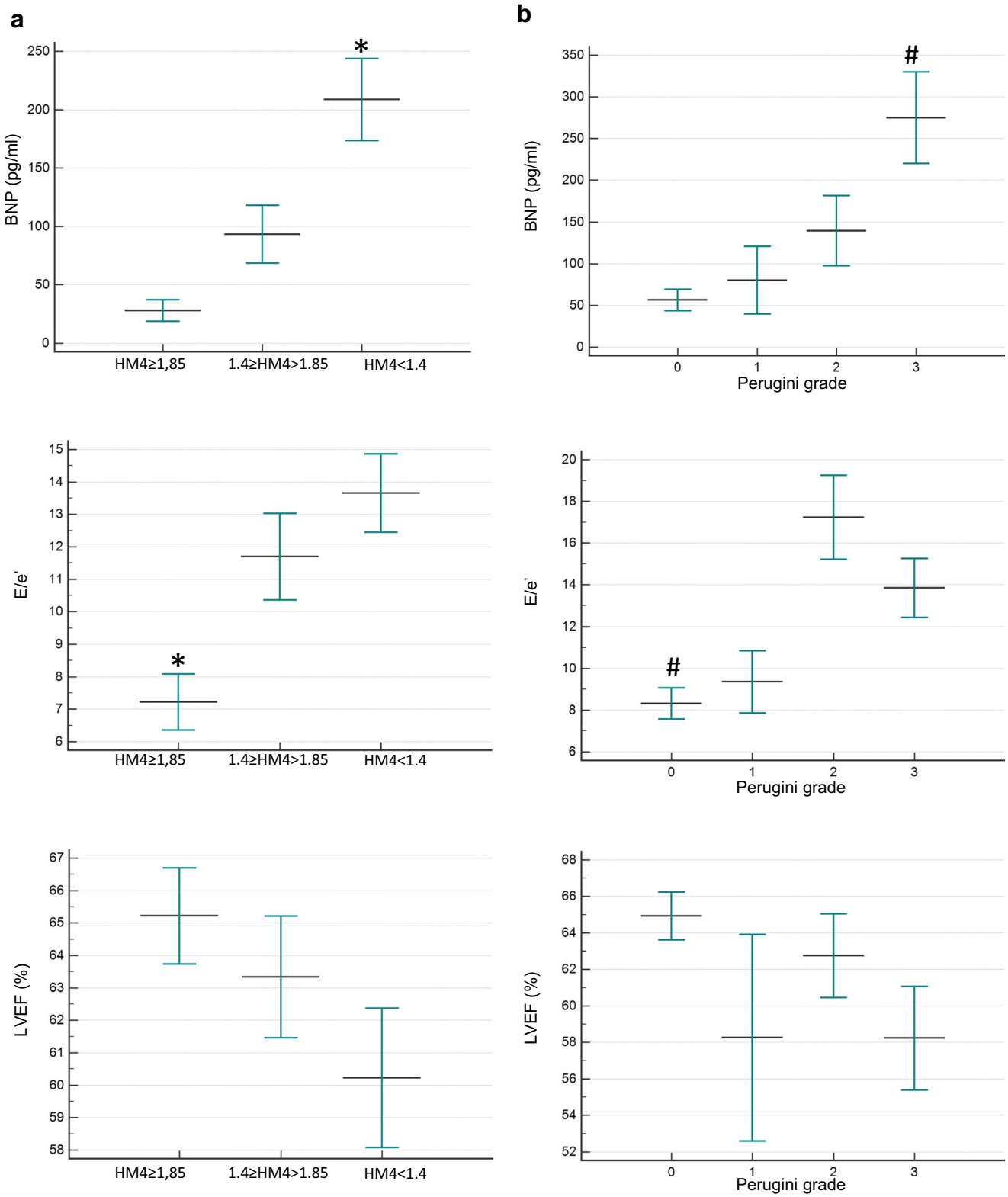

Fig. 5 Selected parameters illustrating cardiac dysfunction according to semi-quantitative uptake intensity of MIBG (column **a**) and DPD (column **b**). * $p < 0.05$ vs the two other groups. # $p < 0.05$ vs the two other groups (except Perugini 1). There were significant differences between the MIBG subgroups (column **a**) with regard to BNP and E/e' (subgroups HM4 ≥ 1.85, 1.85 > HM4 ≥ 1.4 and HM4 < 1.4 respectively; BNP = 28 ± 43 vs 102 ± 120 vs 208 ± 165, $p = 0.0001$; and E/e' = 7.2 ± 4.2 vs 11.6 ± 6.8 vs 14.2 ± 5.6, $p < 0.0001$) but no differences with regard to LVEF (65 ± 7 vs 63 ± 9 vs 60 ± 10, $p = 0.2$)

Table 4 Asymptomatic patients ($n = 31$)

	MIBG normal ($n = 16$)	MIBG abnormal ($n = 15$)	P value
Age [range]	43 ± 10 [30 – 73]	59 ± 16 [30 – 85]	0.001
Males, *n* (%)	11 (69)	9 (60)	0.7
Val30Met, *n* (%)	3 (19)	7 (47)	0.1
DLT, *n* (%)	0	2 (7)	0.2
Amyloidosis targeted therapy			
– Tafamidis / siRNA	1 (6)	3 (20)	0.4
– Liver transplantation	0	1 (7)	0.5
Pacemaker	1 (6)	4 (27)	0.13
Biology			
– BNP > 80 pg/ml	0	6 (40)	0.007
– Troponin > 0.05 µg/l	0	3 (20)	0.1
Echocardiography			
– IVS thickness ≥ 12 mm	2 (13)	8 (53)	0.02
– LVEF < 50%	0	1 (7)	0.5
– GLS (%)	−19.3 ± 1.8	−14.6 ± 6.5	0.03
– E/e' > 13	1 (6)	5 (33)	0.2
DPD scintigraphy			
– positive, *n* (%)	0	7 (47)	0.006
– H/L	0.56 ± 0.20	2.8 ± 2.8	0.003

Values are mean ± SD unless otherwise specified

evaluating myocardial muscarinic receptor density with PET in TTR amyloidosis patients [43] found that FAP patients are also affected by parasympathetic myocardial denervation in a heterogeneous manner, as compared to parasympathetic tone decrease in heart-failure patients. Therefore, we can hypothesize that denervation will occur earlier in the lesser innervated regions, as observed in our study. Those findings suggest that not only do those two pathological mechanisms occur at different stages of the disease, but that they evolve independently.

On regional analysis, we found that two asymptomatic patients presented with segmental denervation on tomographic images, whereas HM4, HM20, and MIBG wash-out rate were within normal ranges. Those patients were considered as true negative of MIBG scintigraphy based on planar findings; however, further longitudinal studies evaluating the evolution of these patients could reveal that tomographic acquisition is more sensitive to detect beginning denervation.

The correlation between age and IVS thickness, and between scintigraphic semi-quantitative parameters (HM20, HM4, MIBG wash-out rate, H/L) and IVS thickness, suggests the role of the exposure duration and amyloid burden in the positivity of scintigraphic examinations. Correlation between diphosphonate scintigraphy and IVS thickness had already been described [27, 28, 31, 44].

Interestingly, two patients presented with a reverse scintigraphic pattern consisting of normal MIBG and markedly positive DPD. Although one of them had mildly increased septum thickness, none had increased filling pressure or abnormal biological markers. Both had very rare mutations: Arg34Gly [45] and Ala36Pro [46–50] presenting with ophthalmic symptomatology, without cardiac nor neurologic symptoms.

Study limitations

Endomyocardial biopsy, which is the gold standard for cardiac amyloidosis, is an invasive and potentially harmful technique and is not performed on a routine basis in our center, and not ethically justified when patients are asymptomatic with normal multimodality imaging. However, the main purpose of our study was to compare the chronological relation between nuclear imaging approaches rather than to compare their diagnostic abilities which have already been reported [14, 15, 19, 20]. Also, MRI findings were not included in the characterization of CA due to substantial methodological and industrial changes throughout the study duration. In the future, advanced MRI sequences should be part of a comprehensive evaluation of CA.

We acknowledge that the results presented here may not apply in a different study population, particularly for TTR gene mutations associated with exclusively cardiac involvement such as Val122Ile. However, based on the results of the THAOS registry our study population matches with the reported distribution of mutations in patients investigated in centers outside the United States with a predominance of Val30Met [51].

Conclusion

The present study shows that in TTR mutation carriers, cardiac sympathetic denervation evidenced by decreased MIBG uptake is detected earlier than amyloid burden evidenced by DPD, although both are related to the patient's age. MIBG and diphosphonate scintigraphy are complementary non-invasive explorations that allow for diagnosis and evaluation of cardiac involvement in hereditary TTR amyloidosis. These results raise the possibility of a diagnostic role for MIBG scintigraphy at an early stage of cardiac involvement in TTR mutated carriers, in addition to its well-established prognostic value. Conversely, DPD uptake, strongly related to patients' age and associated with mild LV systolic dysfunction, seems to be a marker of disease severity.

Funding This study has been supported by the Association Française Contre l'Amylose.

Compliance with ethical standards

Conflict of interest The authors declare that they have no conflict of interest.

References

1. Andrade C. A peculiar form of peripheral neuropathy. Familiar atypical generalized amyloidosis with special involvement of peripheral nerves. Brain. 1952;75:408–26.
2. Adams D, Cauquil C, Labeyrie C, Beaudonnet G, Algalarrondo V, Théaudin M. TTR kinetic stabilizers and TTR gene silencing:a new era in therapy for familial amyloidotic polyneuropathies. Expert Opin Pharmacother. 2016;17(6):791–802.
3. Ericzon BG, Wilczek HE, Larsson M, Wijayatunga P, Stangou A, Pena JR, et al. Liver transplantation for hereditary transthyretin amyloidosis: after 20 years still the best therapeutic alternative? Transplantation. 2015;99(9):1847–54.
4. Coelho T, Maia LF, Martins da Silva A, Waddington Cruz M, Planté-Bordeneuve V, Lozeron P, et al. Tafamidis for transthyretin familial amyloid polyneuropathy: a randomized, controlled trial. Neurology. 2012;79(8):785–92.
5. Adams D, Suhr OB, Dyck PJ, Litchy WJ, Leahy RG, Chen J, et al. Trial design and rationale for APOLLO, a phase 3, placebo-controlled study of patisiran in patients with hereditary ATTR amyloidosis with polyneuropathy. BMC Neurol. 2017 Sep 11;17(1):181.
6. Benson MD, Dasgupta NR, Rissing SM, Smith J, Feigenbaum H. Safety and efficacy of a TTR specific antisense oligonucleotide in patients with transthyretin amyloid cardiomyopathy. Amyloid. 2017 Dec;24(4):219–25.
7. Castano A, Drachman BM, Judge D, Maurer MS. Natural history and therapy of TTR-cardiac amyloidosis: emerging disease-modifying therapies from organ transplantation to stabilizer and silencer drugs. Heart Fail Rev. 2015;20(2):163–78.
8. Arbustini E, Merlini G. Early identification of transthyretin-related hereditary cardiac amyloidosis. J Am Coll Cardiol Img. 2014;7(5):511–4.
9. Wechalekar AD, Gillmore JD, Hawkins PN. Systemic amyloidosis. Lancet. 2016;387(10038):2641–54.
10. Algalarrondo V, Piekarski E, Eliahou L, Le Guludec D, Slama MS, Rouzet F. Can nuclear imaging techniques predict patient outcome and guide medical management decisions in hereditary transthyretin cardiac amyloidosis? Curr Cardiol Rep. In press.
11. Minutoli F, Di Bella G, Mazzeo A, Donato R, Russo M, Scribano E, et al. Comparison between (99m)Tc-diphosphonate imaging and MRI with late gadolinium enhancement in evaluating cardiac involvement in patients with transthyretin familial amyloid polyneuropathy. AJR Am J Roentgenol. 2013;200(3):W256–65.
12. Gertz MA, Benson MD, Dyck PJ, Grogan M, Coelho T, Cruz M, et al. Diagnosis, prognosis, and therapy of transthyretin amyloidosis. J Am Coll Cardiol. 2015;66(21):2451–66.
13. Phelan D, Collier P, Thavendiranathan P, Popović ZB, Hanna M, Plana JC, et al. Relative apical sparing of longitudinal strain using two-dimensional speckle-tracking echocardiography is both sensitive and specific for the diagnosis of cardiac amyloidosis. Heart. 2012;98(19):1442–8.
14. Rapezzi C, Quarta CC, Guidalotti PL, Longhi S, Pettinato C, Leone O, et al. Usefulness and limitations of 99mTc-3,3-diphosphono-1,2-propanodicarboxylic acid scintigraphy in the aetiological diagnosis of amyloidotic cardiomyopathy. Eur J Nucl Med Mol Imaging. 2011;38(3):470–8.
15. Gillmore JD, Maurer MS, Falk RH, Merlini G, Damy T, Dispenzieri A, et al. Nonbiopsy diagnosis of cardiac transthyretin amyloidosis. Circulation. 2016;133(24):2404–12.
16. Castano A, Haq M, Narotsky DL, Goldsmith J, Weinberg RL, Morgenstern R, et al. Multicenter study of planar technetium 99m pyrophosphate cardiac imaging: predicting survival for patients with ATTR cardiac amyloidosis. JAMA Cardiol. 2016;1(8):880–9.
17. Hutt DF, Quigley AM, Page J, Hall ML, Burniston M, Gopaul D, et al. Utility and limitations of 3,3-diphosphono-1,2-propanodicarboxylic acid scintigraphy in systemic amyloidosis. Eur Heart J Cardiovasc Imaging. 2014;15(11):1289–98.
18. Haq M, Pawad S, Berk JL, Miller EJ, Ruberg FL. Can 99m-Tc-pyrophosphate aid in early detection of cardiac involvement in asymptomatic variant TTR amyloidosis? J Am Coll Cardiol Img. 2017;10(6):713–4.
19. Coutinho MC, Cortez-Dias N, Cantinho G, Conceição I, Oliveira A, Bordalo e Sá A, et al. Reduced myocardial 123-iodine metaiodobenzylguanidine uptake: a prognostic marker in familial amyloid polyneuropathy. Circ Cardiovasc Imaging. 2013;6(5):627–36.
20. Algalarrondo V, Antonini T, Théaudin M, Chemla D, Benmalek A, Lacroix C, et al. Cardiac Dysautonomia predicts long-term survival in hereditary transthyretin amyloidosis after liver transplantation. J Am Coll Cardiol Img. 2016;9(12):1432–41.
21. Bechiri MY, Eliahou L, Rouzet F, Fouret PJ, Antonini T, Samuel D, et al. Multimodality imaging of cardiac transthyretin amyloidosis 16 years after a domino liver transplantation. Am J Transplant. 2016;16(7):2208–12.
22. Cohen-Solal A, Rouzet F, Berdeaux A, Le Guludec D, Abergel E, Syrota A, et al. Effects of carvedilol on myocardial sympathetic innervation in patients with chronic heart failure. J Nucl Med. 2005;46(11):1796–803.
23. Perugini E, Guidalotti PL, Salvi F, Cooke RM, Pettinato C, Riva L, et al. Noninvasive etiologic diagnosis of cardiac amyloidosis using 99mTc-3,3-diphosphono-1,2-propanodicarboxylic acid scintigraphy. J Am Coll Cardiol. 2005;46(6):1076–84.
24. Longhi S, Guidalotti PL, Quarta CC, Gagliardi C, Milandri A, Lorenzini M, et al. Identification of TTR-related subclinical amyloidosis with 99mTc-DPD scintigraphy. J Am Coll Cardiol Img. 2014;7(5):531–2.
25. Pilebro B, Suhr OB, Näslund U, Westermark P, Lindqvist P, Sundström T. (99m)Tc-DPD uptake reflects amyloid fibril composition in hereditary transthyretin amyloidosis. Ups J Med Sci. 2016;121(1):17–24.

26. Rossi P, Tessonnier L, Frances Y, Mundler O, Granel B. 99mTc DPD is the preferential bone tracer for diagnosis of cardiac transthyretin amyloidosis. Clin Nucl Med. 2012;37(8):e209–10.
27. Rapezzi C, Quarta CC, Guidalotti PL, Pettinato C, Fanti S, Leone O, et al. Role of 99mTc-DPD Scintigraphy in diagnosis and prognosis of hereditary transthyretin-related cardiac amyloidosis. J Am Coll Cardiol Img. 2011;4(6):659–70.
28. Glaudemans AW, van Rheenen RW, van den Berg MP, Noordzij W, Koole M, Blokzijl H, et al. Bone scintigraphy with (99m)technetium-hydroxymethylene diphosphonate allows early diagnosis of cardiac involvement in patients with transthyretin-derived systemic amyloidosis. Amyloid. 2014;21(1):35–44.
29. Di Bella G, Minutoli F, Piaggi P, Casale M, Mazzeo A, Zito C, et al. Quantitative comparison between amyloid deposition detected by 99mTc-diphosphonate imaging and myocardial deformation evaluated by strain echocardiography in transthyretin-related cardiac amyloidosis. Circ J. 2016;80(9):1998–2003.
30. Moore PT, Burrage MK, Mackenzie E, Law WP, Korczyk D, Mollee P. The utility of 99mTc-DPD scintigraphy in the diagnosis of cardiac amyloidosis: an Australian experience. Heart Lung Circ. 2017; https://doi.org/10.1016/j.hlc.2016.12.017.
31. Galat A, Rosso J, Guellich A, Van Der Gucht A, Rappeneau S, Bodez D, et al. Usefulness of 99mTc-HMDP scintigraphy for the etiologic diagnosis and prognosis of cardiac amyloidosis. Amyloid. 2015;22(4):210–20.
32. Castaño A, DeLuca A, Weinberg R, Pozniakoff T, Blaner WS, Pirmohamed A, et al. Serial scanning with technetium pyrophosphate (99mTc-PYP) in advanced ATTR cardiac amyloidosis. J Nucl Cardiol. 2016;23(6):1355–63.
33. Coutinho CA, Conceição I, Almeida A, Cantinho G, Sargento L, Vagueiro MC. Early detection of sympathetic myocardial denervation in patients with familial amyloid polyneuropathy type I. Rev Port Cardiol. 2004;23(2):201–11.
34. Tanaka M, Hongo M, Kinoshita O, Takabayashi Y, Fujii T, Yazaki Y, et al. Iodine-123 metaiodobenzylguanidine scintigraphic assessment of myocardial sympathetic innervation in patients with familial amyloid polyneuropathy. J Am Coll Cardiol. 1997;29:168–74.
35. Takahashi R, Ono K, Shibata S, Nakamura K, Komatsu J, Ikeda Y, et al. Efficacy of diflunisal on autonomic dysfunction of late-onset familial amyloid polyneuropathy (TTR Val30Met) in a Japanese endemic area. J Neurol Sci. 2014;345(1-2):231–5.
36. Sperry BW, Vranian MN, Tower-Rader A, Hachamovitch R, Hanna M, Brunken R, et al. Regional variation in technetium pyrophosphate uptake in transthyretin cardiac amyloidosis and impact on mortality. J Am Coll Cardiol Img. 2018;11(2 Pt 1):234-42
37. Le Guludec D, Delforge J, Dolle F. Imaging the parasympathetic cardiac innervation with PET. In: Slart R, Tio R, Elsinga P, Schwaiger M, editors. Autonomic innervation of the heart. Berlin: Springer; 2015.
38. Kawano H, Okada R, Yano K. Histological study on the distribution of autonomic nerves in the human heart. Heart Vessel. 2003;18:32–9.
39. Gill JS, Hunter GJ, Gane G, Camm AJ. Heterogeneity of the human myocardial sympathetic innervation: in vivo demonstration by iodine 123-labeled meta-iodobenzylguanidine scintigraphy. Am Heart J. 1993;126(2):390–8.
40. Delahaye N, Dinanian S, Slama MS, Mzabi H, Samuel D, Adams D, et al. Cardiac sympathetic denervation in familial amyloid polyneuropathy assessed by iodine-123 metaiodobenzylguanidine scintigraphy and heart rate variability. Eur J Nucl Med. 1999 Apr;26(4):416–24.
41. Delahaye N, Rouzet F, Sarda L, Tamas C, Dinanian S, Plante-Bordeneuve V, et al. Impact of liver transplantation on cardiac autonomic denervation in familial amyloid polyneuropathy. Medicine (Baltimore). 2006 Jul;85(4):229–38.
42. Algalarrondo V, Eliahou L, Thierry I, Bouzeman A, Dasoveanu M, Sebag C, et al. Circadian rhythm of blood pressure reflects the severity of cardiac impairment in familial amyloid polyneuropathy. Arch Cardiovasc Dis. 2012 May;105(5):281–90. https://doi.org/10.1016/j.acvd.2012.03.004.
43. Delahaye N, Le Guludec D, Dinanian S, Delforge J, Slama MS, Sarda L, et al. Myocardial muscarinic receptor upregulation and normal response to isoproterenol in denervated hearts by familial amyloid polyneuropathy. Circulation. 2001 Dec 11;104(24):2911–6.
44. Kristen AV, Scherer K, Buss S, aus dem Siepen F, Haufe S, Bauer R, et al. Noninvasive risk stratification of patients with transthyretin amyloidosis. J Am Coll Cardiol Img. 2014;7(5):502–10.
45. Levy J, Hawkins PN, Rowczenio D, Godfrey T, Stawell R, Zamir E. Familial amyloid polyneuropathy associated with the novel transthyretin variant Arg34Gly. Amyloid. 2012;19(4):201–3.
46. Jones LA, Skare JC, Harding JA, Cohen AS, Milunsky A, Skinner M. Proline at position 36: a new transthyretin mutation associated with familial amyloidotic polyneuropathy. Am J Hum Genet. 1991;48(5):979–82.
47. Jacobson DR, Rosenthal CJ, Buxbaum JN. Transthyretin pro 36 associated with familial amyloidotic polyneuropathy in an Ashkenazic Jewish kindred. Hum Genet. 1992;90(1-2):158–60.
48. Chaves M, Bettini M, Marciano S, Sáez S, Cristiano E, Rugiero M. Presentations of transthyretin associated familial amyloid polyneuropathy in Argentina. Medicina (B Aires). 2016;76(2):105–8.
49. Zou X, Dong F, Zhang S, Tian R, Sui R. Transthyretin Ala36Pro mutation in a Chinese pedigree of familial transthyretin amyloidosis with elevated vitreous and serum vascular endothelial growth factor. Exp Eye Res. 2013; https://doi.org/10.1016/j.exer.2013.02.005.
50. Meng LC, Lyu H, Zhang W, Liu J, Wang ZX, Yuan Y. Hereditary transthyretin amyloidosis in eight Chinese families. Chin Med J. 2015; https://doi.org/10.4103/0366-6999.168048.
51. Maurer MS, Hanna M, Grogan M, Dispenzieri A, Witteles R, Drachman B, et al. Genotype and phenotype of transthyretin cardiac amyloidosis: THAOS (Transthyretin Amyloid Outcomes Survey). J Am Coll Cardiol. 2016;68(2):161–72.